Near-Infrared Fluorescence (NIRF) Imaging in Breast-Conserving Surgery: Assessing Intraoperative Techniques in Tissue-Simulating Breast Phantoms

R.G. Pleijhuis, G.C. Langhout, W. Helfrich, G. Themelis, A. Sarantopoulos, L.M.A. Crane, N.J. Harlaar, J.S. de Jong, V. Ntziachristos, G.M. van Dam

Accepted Manuscript

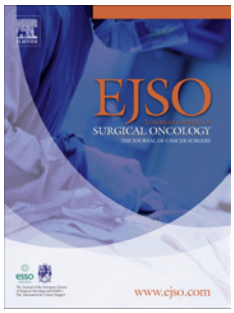

Title: Near-Infrared Fluorescence (NIRF) Imaging in Breast-Conserving Surgery: Assessing Intraoperative Techniques in Tissue-Simulating Breast Phantoms

Authors: R.G. Pleijhuis, G.C. Langhout, W. Helfrich, G. Themelis, A. Sarantopoulos, L.M.A. Crane, N.J. Harlaar, J.S. de Jong, V. Ntziachristos, G.M. van Dam

PII: S0748-7983(10)00548-2

DOI: 10.1016/j.ejso.2010.10.006

Reference: YEJSO 3063

To appear in: *European Journal of Surgical Oncology*

Received Date: 11 July 2010

Revised Date: 28 September 2010

Accepted Date: 26 October 2010

Please cite this article as: Pleijhuis RG, Langhout GC, Helfrich W, Themelis G, Sarantopoulos A, Crane LMA, Harlaar NJ, de Jong JS, Ntziachristos V, van Dam GM. Near-Infrared Fluorescence (NIRF) Imaging in Breast-Conserving Surgery: Assessing Intraoperative Techniques in Tissue-Simulating Breast Phantoms, European Journal of Surgical Oncology (2010), doi: 10.1016/j.ejso.2010.10.006

Near-Infrared Fluorescence (NIRF) Imaging in Breast-Conserving Surgery: Assessing Intraoperative Techniques in Tissue-Simulating Breast Phantoms

R.G. Pleijhuis[1,2], G.C. Langhout[1,2], W. Helfrich[1,2], G. Themelis[3], A. Sarantopoulos[3], L.M.A. Crane[1,2], N.J. Harlaar[1,2], J.S. de Jong[2,4], V. Ntziachristos[3], and G.M. van Dam[1,2]

[1]*Department of Surgery, University Medical Center Groningen, Groningen, The Netherlands*

[2]*BioOptical Imaging Center, University Medical Center Groningen, Groningen, The Netherlands*

[3]*Institute for Biological and Medical Imaging, Helmholtz Zentrum München / Technische Universität München, Munich, Germany*

[4]*Department of Surgery, Erasmus Medical Center, Rotterdam, The Netherlands*

Corresponding author:
Gooitzen M. van Dam, MD, PhD
Department of Surgery, BioOptical Imaging Center Groningen
University Medical Center Groningen
Hanzeplein 1
9700 RB Groningen
The Netherlands
Tel.: +31-50-3612283
Fax: +31-50-3614873
E-mail: g.m.van.dam@chir.umcg.nl

Key words:
Human breast cancer; near-infrared fluorescence; tissue-simulating phantoms; intraoperative imaging.

Running head:
NIRF imaging in tissue-simulating breast phantoms

Synopsis:
Near-infrared fluorescence (NIRF)-based tumour imaging has great potential for improving breast-conserving surgery. In this report, intraoperative NIRF applications were pre-clinically evaluated using tissue-simulating breast phantoms equipped with fluorescent tumour-like inclusions of different size and shape in breast-conserving surgery simulations.

Abstract

Purpose:

Breast-conserving surgery (BCS) results in tumour-positive surgical margins in up to 40% of the patients. Therefore, new imaging techniques are needed that support the surgeon with real-time feedback on tumour location and margin status. In this study, the potential of near-infrared fluorescence (NIRF) imaging in BCS for pre- and intraoperative tumour localization, margin status assessment and detection of residual disease was assessed in tissue-simulating breast phantoms.

Methods:

Breast-shaped phantoms were produced with optical properties that closely match those of normal breast tissue. Fluorescent tumour-like inclusions containing ICG were positioned at predefined locations in the phantoms to allow for simulation of i) preoperative tumour localization, ii) real-time NIRF-guided tumour resection, and iii) intraoperative margin assessment. Optical imaging was performed using a custom-made clinical prototype NIRF intraoperative camera.

Results:

Tumour-like inclusions in breast phantoms could be detected up to a depth of 21 mm using a NIRF intraoperative camera system. Real-time NIRF-guided resection of tumour-like inclusions proved feasible. Moreover, intraoperative NIRF imaging reliably detected residual disease in case of inadequate resection.

Conclusion:

We evaluated the potential of NIRF imaging applications for BCS. The clinical setting was simulated by exploiting tissue-like breast phantoms with fluorescent tumour-like agarose inclusions. From this evaluation, we conclude that intraoperative NIRF imaging is feasible and may improve BCS by providing the surgeon with imaging information on tumour location, margin status, and presence of residual disease in real-time. Clinical studies are needed to further validate these results.

Introduction

Breast cancer is the most frequent malignancy in women worldwide with an estimated 1.4 million new cases in 2010 (1). Breast-conserving therapy (BCT), consisting of breast-conserving surgery (BCS) followed by radiation therapy, has become the standard treatment for T1-T2 breast tumours and is generally regarded as sufficient for this subset of patients (2). Unfortunately, a majority of studies on the surgical margin status after BCS have shown that positive margins are detected in 20 to 40% of patients, necessitating additional surgical intervention or radiotherapy (3). Two major points for improving outcome after BCS involve i) a more reliable intraoperative tumour localization and ii) improved real-time feedback on the presence of possible residual disease during or after excision of the tumour (4). Intraoperative application of an optical imaging technique known as *near-infrared fluorescence* (NIRF) imaging may improve the clinical outcome of BCS (3;5).

Near-infrared fluorescence imaging

In recent years, significant progress has been made in the development of optical imaging systems and fluorophores for clinical applications (6;7). Several animal (5;8-10) and clinical (11-15) studies have shown the potential clinical use of NIRF imaging to improve the therapeutic outcome of surgery. Compared to light in the visible spectral range (400-650 nm), application of near-infrared (NIR) light minimizes absorption by physiologically abundant molecules such as hemoglobin and lipids, which increases penetration depth (16;17). Additionally, autofluorescence (the intrinsic fluorescence signal present in all living cells due to various normal metabolites and tissue constituents) is strongly reduced in the NIR spectral range. Taken together, these aspects of NIR light make it particularly suitable for use in

intraoperative optical imaging applications. However, clinical application of NIRF imaging in BCS is currently limited to the non-specific intraoperative detection of the sentinel lymph node (11;12;14;18-20).

Tumour-targeted near-infrared fluorophores

With the introduction of clinical grade tumour-targeted NIR fluorophores, NIRF imaging may be extended towards the intraoperative detection of the primary tumour (10). Several target molecules have been indentified for breast cancer that may be of value for such an approach, including Her2/neu receptor (9;21;22), vascular endothelial growth factor (VEGF) receptor (23;24), endothelial growth factor (EGF) receptor (25) and folate receptor-α (26).

In tumour-targeted NIRF imaging, a tumour-targeted NIR fluorophore is administered several hours or days prior to the imaging procedure. Subsequently, an external laser is used to irradiate the breast with light in the NIR spectral range (650-900 nm) (17). Upon excitation, the fluorophore will release photons of a higher NIR wavelength. Because NIR light is invisible to the naked eye, a dedicated optical imaging system is necessary to capture the NIR signal from the surgical field and digitally convert it to a visible image. Recently, we and our co-workers developed a multispectral NIRF intraoperative camera system that is suitable for intraoperative use with NIR fluorophores (27).

Simulation of NIRF-guided breast-conserving surgery

In the current preclinical study, we evaluated intraoperative NIRF imaging applications in a simulated clinical setting as a step-up toward NIRF-guided BCS. To this end, we used tissue-simulating gelatin-based breast phantoms that mimic the

optical properties of normal breast tissue (28;29). Tumour-like fluorescent inclusions of different size and shape were positioned at predefined sites in the phantoms, allowing for simulation of i) preoperative tumour localization, ii) real-time NIRF-guided tumour resection and iii) intraoperative macroscopic margin assessment. The tumor-like inclusions contain the non-specific NIR fluorophore indocyanine green (ICG), to simulate for the use of tumour-targeted near-infrared fluorophores in BCS. Currently, ICG (absorption and emission maximum at ~780 and ~820 nm, respectively) is one of the few FDA-approved NIR fluorophores available for clinical use (9). Sevick-Muraca et al. have previously shown the feasibility of NIRF imaging following microdose administration of ICG (12). Although ICG in itself is non-specific, their findings suggest that comparable microdose concentrations can be used to label cancer cells with tumour-targeted NIR fluorophores for intraoperative NIRF imaging. Importantly, new fluorophores in the NIR spectral range are currently being developed, e.g. IRDye® 800CW, with properties more promising for intraoperative use compared to ICG (25).

Material and Methods

Assessment of ICG fluorescence self-quenching in agarose

Because increasing concentrations of ICG may not correspond to an increased fluorescence signal due to self-quenching of ICG, different concentrations of ICG in agarose were evaluated for fluorescence activity (29;30). Briefly, an ICG stock solution was serially diluted in 10 ml sterile water (ranging from 0.5 uM to 350 uM ICG), after which 2% agarose was added. The mixture was then heated to 70℃ and stirred until the agarose was completely dissolved. After solidification of the agarose mixture for 15 min at 4℃, fluorescence reflectance imaging (FRI) was performed to determine maximum photon counts/sec (settings: exposure time: 1000 ms, excitation: 780 nm, emission: 820 nm).

Assessment maximal penetration depth of ICG fluorescence

In order to determine the maximal penetration depth of the NIRF signal, a cubic fluorescent inclusion of 5x5x5 mm containing 14 µM ICG was positioned in phantom tissue at a depth of 30 mm. Subsequently, the surgeon excised 3-4 mm layers of phantom towards the inclusion (remaining depths were 27, 24, 21, 18, 15, 11, 7, and 4 mm, respectively). At all depths, FRI was performed with the intraoperative NIRF camera system (exposure time: 3000-60000 ms, excitation 780 nm, emission 820 nm, binning: small-medium). Maximum photon counts per second exposure time were calculated as well as the full width at half maximum (FWHM) of the fluorescence signal. The FWHM is a measure for scattering and indicates the diameter of the fluorescence signal when the intensity of the signal is reduced to half the maximum. Scattering both contributes to signal loss and loss in resolution. The

FWHM indicates the minimal distance between two distinct sources to be recognized as separate.

Tissue-Simulating Breast Phantoms

Composition of the tissue-simulating gelatin-based breast phantoms was aimed at obtaining uniform optical properties that closely match the optical characteristics of normal breast tissue, as described in detail before (29). Additionally, the breast phantoms mimic the elastic properties of human tissue (31).

Briefly, 10% gelatin 250 (Natural Spices, Watergang, the Netherlands) was dissolved in 1 l TBS (50 mmol Tris-HCl ,150 mmol NaCl , pH 7.4). To remove molecular oxygen and prevent microbial infection, 15 mmol NaN_3 (Merck, Darmstadt, Germany) was added. The gelatin slurry was completely dissolved by heating to 50℃ and subsequently cooled down to 35℃ and maintained at this temperature. Under constant stirring, 170 µmol hemoglobin (Sigma-Aldrich, Zwijndrecht, The Netherlands) and 1% Intralipid® 20% (Sigma-Aldrich) were added. Next, the gelatin mixture was poured in a custom-made pre-chilled breast-shaped mold (end volume 500 ml) to a level that corresponded to the predefined depth of the agarose inclusion. After solidification for 30 min at 4℃, a tumour-li ke NIR fluorescent agarose inclusion was positioned on the surface and temporarily fixed with a small needle. Next, the remaining of the warmed gelatin mixture was added to fill up the remaining mold volume, allowing for adherence of both layers. The phantom was then stored in the dark to solidify for another 30 min at 4^oC, after which it was gently removed from its mold.

In total, 4 breast phantoms were constructed with tumour-like NIR fluorescent agarose inclusions of different size and shape (figure 1A) positioned at predefined depths. Imaging of the phantoms was performed directly after production of all 4 phantoms.

Breast phantom #1 contained 2 similar-sized (Ø1.0 cm) sphere-shaped agarose inclusions at different depths (2.0 and 4.0 cm). Phantom #2 contained 2 sphere-shaped inclusions at the same depth (1.5 cm), differing in size (Ø 0.5 cm and Ø 2.0 cm). Phantom #3 contained 1 sphere-shaped (Ø1.0 cm) and 1 prolate sphere-shaped (Ø1.0 cm) agarose inclusion at the same depth (1.5 cm). Finally, phantom #4 contained 2 irregular shaped agarose inclusions of similar size (Ø1.5 cm) at different depths (1.5 and 3.0 cm).

Tumour-like NIR fluorescent agarose inclusions

For tumour-like NIR fluorescent agarose inclusions, 2% agarose (Hispanagar, Burgos, Spain) was used instead of 10% gelatin. Agarose has a higher melting point which prevents the inclusions from dissolving and leaking ICG (see below) during and after the positioning procedure in the gelatin phantom. In short, a 2% (W/V) agarose slurry was heated to 70℃ and stirred until the agarose was completely dissolved. Subsequently, ICG (ICG-PULSION®; Pulsion Medical Systems, Munich, Germany) was dissolved to a final concentration of 14 µM. Finally, in order to resemble the optical appearance of the surrounding breast phantom tissue, 170 µM hemoglobin,15 mM NaN_3 and 1% Intralipid® 20% were added to the tumour-like fluorescent inclusions.

Tumour-like fluorescent inclusions of different size (range: 0.5 cm to 2.0 cm) and shape (prolate sphere, sphere and irregular shape, Figure 1A) were produced. The

inclusions were integrated in the breast phantoms as indicated and chilled in the dark for 30 min at 4℃. Imaging of each individual breast phantom was performed within 6 h.

Near-infrared fluorescence imaging system

A custom-made NIRF camera system was developed in collaboration with SurgOptix Inc (SurgOptix Inc, Redwood Shores CA, USA) for real-time intraoperative imaging. The system implements a correction scheme that improves the accuracy of epi-illumination fluorescence images for light intensity variations in tissue. Implementation is based on the use of three cameras operating in parallel. The camera is mounted on a five degrees of freedom bracket, the sixth degree (rotation) can be performed digitally. This camera allows for simultaneous acquisition of colour videos and normalized fluorescence images in real-time, yielding a lateral resolution up to 66.58 µm and a variable field of view (FOV) of 13.5W x 11H to 115W x 95H (mm). A description in full detail is provided by Themelis et al (27). The invisible NIRF imaging signal was digitally converted into a pseudo-colour and superposed on a colour video image of the operating field, allowing for real-time, intraoperative anatomical positioning of the fluorescence signal.

Simulation of intraoperative NIRF imaging

Breast phantoms with tumour-like NIR fluorescent agarose inclusions were used to simulate and evaluate the potential of NIRF imaging applications in BCS (Figure 1 and 3). In all phantoms, the location of the tumour-like fluorescent inclusions was assessed preoperatively with non-invasive NIRF imaging. In phantoms #1 and #2, the tumour-like fluorescent inclusions were subsequently excised using conventional

surgical equipment, guided solely by visual inspection, tactile information, and preoperatively obtained NIRF imaging data. The surgeon was asked to indicate when he believed a complete excision of the tumour was reached. Subsequently, the NIRF camera system was applied to assess the feasibility of NIRF-guided macroscopic margin assessment of the surgical cavity and excised tissue fragments. In case of an incomplete excision, the surgeon was asked to perform a re-excision under real-time NIRF-guidance.

In phantoms #3 and #4, the tumour-like fluorescent inclusions were localized and excised under real-time NIRF guidance. While approaching the tumour-like fluorescent inclusions, the surgeon was supported with both visible and audible information. In short, the detected fluorescent signal was depicted on a TFT-screen and was made quantitatively audible using a digitally generated sound-pitch. In this approach, an increase in sound-pitch represents an increase in fluorescence signal indicating the approximation of a tumour-like fluorescent inclusion.

Results

ICG fluorescence self-quenching in agarose

To determine the optimal ICG concentration in agarose, a serial range of increasing ICG concentrations was analyzed for fluorescence characteristics. The optimal fluorescence signal was observed at a concentration of approximately 10 µM ICG (Figure 4). These results are comparable to self-quenching characteristics of ICG as previously determined in gelatin (29).

Maximal penetration depth of ICG fluorescence

The maximal tissue penetration depth of a detectable fluorescent ICG inclusion was reached at a depth of 21 mm (Figure 2C and supplemental video 2).

Simulation of intraoperative NIRF imaging

Preoperative NIRF-guided localization of tumour-like fluorescent agarose inclusions was performed in 4 different breast phantoms. The various tumour-like inclusions positioned at a depth of ≤ 2.0 cm were detectable with the NIRF camera system (figure 3A-I). Tumour-like inclusions positioned at depths of 3.0 and 4.0 cm could not be detected preoperatively.

Tumour-like inclusions in phantom #1 and #2 were excised using conventional techniques for tumour localization. In phantom #1, one out of two tumour-like inclusions proved to be only partially excised, as evidenced by a remnant strong fluorescence signal in the surgical cavity detected by the NIRF camera system (figure 3C-III). In phantom #2, the excision of one out of two inclusions was found to be incomplete. In case of residual fluorescence, the surgeon could detect and excise (theranostic procedure) the remnant inclusion under real-time NIRF guidance (figure 3C-IV and supplemental video 1). In all cases, NIRF-guided re-excision resulted in a complete excision, without the need for additional excision of large breast phantom fragments (figure 3C-V).

In phantoms #3 and #4, the tumour-like inclusions were located (figure 3B) and excised (figure 3C) under real-time NIRF-guidance. Although the inclusion at 3.0 cm depth in phantom #4 could not be detected preoperatively (figure 3B-I), it was detectable using the NIRF camera system after an incision of approximately 1 cm of superficial phantom tissue (figure 3B-II). In phantom #3, no residual tumour-like inclusion material could be detected after initial NIRF-guided excision, while the excision of one out of two irregular inclusions in phantom #4 was found to be incomplete. Again, subsequent NIRF-guided re-excision resulted in a complete excision.

During the surgical simulation procedure, the approximation of the surgeon towards tumour-like fluorescent agarose inclusions was guided by both visual information on a TFT screen and audible sound-pitched information (Supplemental videos 1-2). The approach resulted in a clear change in the signal strength of the fluorescence image that was accompanied with an increase of the sound pitch at ~15 mm prior to excision of the tumour-like agarose inclusion. These signals assisted the surgeon in carefully advancing the margins.

Discussion

Tissue-like phantoms and tumour-like inclusions

The composition of the breast phantoms was based on data published by De Grand et al, who developed and validated phantoms to mimic the basic optical characteristics (absorption and scattering coefficients) of breast tissue(29). The absorption of photons by both cellular organelles and blood was simulated by hemoglobin, which gives the phantoms a deep red colour (32;33). Additionally, Intralipid® was added to mimic scattering properties of breast tissue (28).

In order to resemble the clinical situation as close as possible, tumour-like fluorescent agarose inclusions were incorporated in the breast phantoms. The agarose-based inclusions simulate the firm-elastic consistency of tumour tissue and allow for surgical margin status assessment, both intraoperatively (NIRF-guided surgery) and *ex vivo* (NIRF-guided macroscopic margin assessment). The relatively low concentration of ICG used in this study resembles the potential application of microdose tumour-targeted fluorophores (ranging from 1 to 100 µM) in BCS.

Although the phantoms used in this study are homogeneous, and therefore do not possess the complex structures that characterize mammary tissue, they do provide a tool for assessing the value of theoretical assumptions and indicate generally important features of future clinical NIRF imaging applications in BCS.

Near-infrared fluorescence imaging: strengths and drawbacks

NIRF imaging offers a promising technique for real-time NIRF-guided surgery in BCS with little interference in the standard surgical procedure or changes in the design of the operating theatre. The technology is considered safe, fast, makes use of non-

ionizing radiation, and has a high resolution (3;10). However, NIRF imaging does have limitations originating from the intrinsic characteristics of light propagation through tissue, including scattering and absorbance (17).

Additionally, due to limited depth resolution and a non-linear dependence of the signal detected and the depth of the fluorescence activity, NIRF imaging by epi-illumination with our current camera system seems of limited value for preoperative localization of tumours. This applies in particular to situations where the tumour is located relatively deep (> 2 cm) in fat and glandular tissue of the breast. However, since the surgeon, by definition, will bring the area of interest closer to the surface during surgery, our multispectral NIRF camera system is well-suited for intraoperative imaging applications.

NIRF imaging instruments designed for preoperative imaging, e.g. the SoftScan (ART, Advanced Research Technologies, Saint-Laurent (Quebec), Canada), show penetration depths far superior (up to 15 cm) to intraoperative imaging systems (34). This difference in penetration depth is due to the application of different imaging strategies which are largely incompatible with surgery, e.g. trans-illumination and the need for light conduction liquid media.

Non-specific versus tumour-targeted fluorophores

Several possibilities exist for delivering fluorophores to the tumour. One possibility would be to inject a non-specific fluorophore (e.g. ICG) into the tumour under stereotactic or ultrasonographic guidance (35). However, there are some significant drawbacks to this approach. First, the injection of the nonspecific fluorophore into the tumour is a critical step in the procedure and has to be very accurate to minimize false-negative and false-positive results. Additionally, spillage/leakage of fluorophore

within the mammary gland during the procedure will decrease accuracy of both localization of the tumour and macroscopic margin assessment. Therefore, we believe NIRF-guided surgery should ideally be combined with tumour-targeted fluorophores, which provide molecularly-specific detection of cancer cells. In these agents, the NIR fluorophore has been conjugated to a specific targeting ligand or monoclonal antibody. This allows for tumour-specific binding of the fluorophore, increasing SN ratios and minimizing spillage of the fluorophore during the surgical procedure (3;10). Several studies have shown the feasibility of using tumour-targeted fluorophores *in vivo* to image tumours intraoperatively, including the use of tumour-targeted ICG-conjugated agents (5;9;22;25;26;36;37). However, there are some significant drawbacks, including the heterogeneity of (breast) tumours which should be solved before applying tumour-targeted NIRF imaging in the clinic. In BCS, the preoperative biopsy taken prior to surgery could provide important information on molecular targets for NIRF imaging. As this biopsy is considered standard practice, it will not require an additional invasive procedure, while offering the possibility to determine the expression of different kinds of molecular targets present on the breast cancer cells by immunohistochemical analysis. The surgeon could then look for NIRF agents suited for each individual tumour, offering a more patient-tailored approach.

Conclusion

We have pre-clinically assessed the applicability of NIRF imaging applications in BCS by exploiting tissue-simulating breast phantoms. NIRF-guided intraoperative tumour localization and detection of remnant disease showed feasible. Clinical studies are needed to further validate these results for use in BCS.

Acknowledgements

This work was supported by a grant from the Jan Kornelis de Cock foundation. The authors wish to thank Mr. T. Buddingh, MD for assistance in operating on the phantoms.

References

1. Parkin DM, Bray F, Ferlay J, Pisani P. Global Cancer Statistics, 2002. *CA Cancer J Clin* 2005; **55**(2): 74-108.

2. Schwartz GF, Veronesi U, Clough KB, Dixon JM, Fentiman IS, Heywang-Kobrunner SH, Holland R, Hughes KS, Mansel RE, Margolese R, Mendelson EB, Olivotto IA, Palazzo JP, Solin LJ. Consensus Conference on Breast Conservation. *J Am Coll Surg* 2006; **203**(2): 198-207.

3. Pleijhuis RG, Graafland M, de Vries J, Bart J, de Jong JS, van Dam GM. Obtaining Adequate Surgical Margins in Breast-Conserving Therapy for Patients With Early-Stage Breast Cancer: Current Modalities and Future Directions. *Ann Surg Oncol* 2009; **16**(10): 2717-30.

4. Singletary SE. Breast Cancer Surgery for the 21st Century: the Continuing Evolution of Minimally Invasive Treatments. *Minerva Chir* 2006; **61**(4): 333-52.

5. Kirsch DG, Dinulescu DM, Miller JB, Grimm J, Santiago PM, Young NP, Nielsen GP, Quade BJ, Chaber CJ, Schultz CP, Takeuchi O, Bronson RT, Crowley D, Korsmeyer SJ, Yoon SS, Hornicek FJ, Weissleder R, Jacks T. A Spatially and Temporally Restricted Mouse Model of Soft Tissue Sarcoma. *Nat Med* 2007; **13**(8): 992-7.

6. Luker GD, Luker KE. Optical Imaging: Current Applications and Future Directions. *J Nucl Med* 2008; **49**(1): 1-4.

7. Tromberg BJ, Pogue BW, Paulsen KD, Yodh AG, Boas DA, Cerussi AE. Assessing the Future of Diffuse Optical Imaging Technologies for Breast Cancer Management. *Med Phys* 2008; **35**(6): 2443-51.

8. von Burstin J, Eser S, Seidler B, Meining A, Bajbouj M, Mages J, Lang R, Kind AJ, Schnieke AE, Schmid RM, Schneider G, Saur D. Highly Sensitive Detection of Early-Stage Pancreatic Cancer by Multimodal Near-Infrared Molecular Imaging in Living Mice. *Int J Cancer* 2008.

9. Chopra A. Trastuzumab Complexed to Near-Infrared Fluorophore Indocyanine Green. 2004.

10. Keereweer S, Kerrebijn JD, van Driel PB, Xie B, Kaijzel EL, Snoeks TJ, Que I, Hutteman M, van dV, Jr., Mieog JS, Vahrmeijer AL, van d, V, Baatenburg de Jong RJ, Lowik CW. Optical Image-Guided Surgery-Where Do We Stand? *Mol Imaging Biol* 2010.

11. Tagaya N, Yamazaki R, Nakagawa A, Abe A, Hamada K, Kubota K, Oyama T. Intraoperative Identification of Sentinel Lymph Nodes by Near-Infrared Fluorescence Imaging in Patients With Breast Cancer. *Am J Surg* 2008; **195**(6): 850-3.

12. Sevick-Muraca EM, Sharma R, Rasmussen JC, Marshall MV, Wendt JA, Pham HQ, Bonefas E, Houston JP, Sampath L, Adams KE, Blanchard DK, Fisher RE, Chiang SB, Elledge R, Mawad ME. Imaging of Lymph Flow in Breast Cancer Patients After Microdose Administration of a Near-Infrared Fluorophore: Feasibility Study. *Radiology* 2008; **246**(3): 734-41.

13. Brandt MG, Moore CC, Jordan K. Randomized Control Trial of Fluorescence-Guided Surgical Excision of Nonmelanotic Cutaneous Malignancies. *J Otolaryngol* 2007; **36**(3): 148-55.

14. Ogasawara Y, Ikeda H, Takahashi M, Kawasaki K, Doihara H. Evaluation of Breast Lymphatic Pathways With Indocyanine Green Fluorescence Imaging in Patients With Breast Cancer. *World J Surg* 2008; **32**(9): 1924-9.

15. Stummer W, Pichlmeier U, Meinel T, Wiestler OD, Zanella F, Reulen HJ. Fluorescence-Guided Surgery With 5-Aminolevulinic Acid for Resection of Malignant Glioma: a Randomised Controlled Multicentre Phase III Trial. *Lancet Oncol* 2006; **7**(5): 392-401.

16. Bremer C, Ntziachristos V, Weissleder R. Optical-Based Molecular Imaging: Contrast Agents and Potential Medical Applications. *Eur Radiol* 2003; **13**(2): 231-43.

17. Ntziachristos V. Fluorescence Molecular Imaging. *Annu Rev Biomed Eng* 2006; **8**: 1-33.

18. Troyan SL, Kianzad V, Gibbs-Strauss SL, Gioux S, Matsui A, Oketokoun R, Ngo L, Khamene A, Azar F, Frangioni JV. The FLARE Intraoperative Near-Infrared Fluorescence Imaging System: a First-in-Human Clinical Trial in Breast Cancer Sentinel Lymph Node Mapping. *Ann Surg Oncol* 2009; **16**(10): 2943-52.

19. Kitai T, Inomoto T, Miwa M, Shikayama T. Fluorescence Navigation With Indocyanine Green for Detecting Sentinel Lymph Nodes in Breast Cancer. *Breast Cancer* 2005; **12**(3): 211-5.

20. Murawa D, Hirche C, Dresel S, Hunerbein M. Sentinel Lymph Node Biopsy in Breast Cancer Guided by Indocyanine Green Fluorescence. *Br J Surg* 2009; **96**(11): 1289-94.

21. Gee MS, Upadhyay R, Bergquist H, Alencar H, Reynolds F, Maricevich M, Weissleder R, Josephson L, Mahmood U. Human Breast Cancer Tumor Models: Molecular Imaging of Drug Susceptibility and Dosing During HER2/Neu-Targeted Therapy. *Radiology* 2008; **248**(3): 925-35.

22. Lee SB, Hassan M, Fisher R, Chertov O, Chernomordik V, Kramer-Marek G, Gandjbakhche A, Capala J. Affibody Molecules for in Vivo Characterization of HER2-Positive Tumors by Near-Infrared Imaging. *Clin Cancer Res* 2008; **14**(12): 3840-9.

23. Backer MV, Levashova Z, Patel V, Jehning BT, Claffey K, Blankenberg FG, Backer JM. Molecular Imaging of VEGF Receptors in Angiogenic Vasculature With Single-Chain VEGF-Based Probes. *Nat Med* 2007; **13**(4): 504-9.

24. Chen K, Li ZB, Wang H, Cai W, Chen X. Dual-Modality Optical and Positron Emission Tomography Imaging of Vascular Endothelial Growth Factor Receptor on Tumor Vasculature Using Quantum Dots. *Eur J Nucl Med Mol Imaging* 2008; **35**(12): 2235-44.

25. Sampath L, Kwon S, Ke S, Wang W, Schiff R, Mawad ME, Sevick-Muraca EM. Dual-Labeled Trastuzumab-Based Imaging Agent for the Detection of Human Epidermal Growth Factor Receptor 2 Overexpression in Breast Cancer. *J Nucl Med* 2007; **48**(9): 1501-10.

26. Sega EI, Low PS. Tumor Detection Using Folate Receptor-Targeted Imaging Agents. *Cancer Metastasis Rev* 2008; **27**(4): 655-64.

27. Themelis G, Yoo JS, Soh KS, Schulz R, Ntziachristos V. Real-Time Intraoperative Fluorescence Imaging System Using Light-Absorption Correction. *J Biomed Opt* 2009; **14**(6): 064012.

28. Pogue BW, Patterson MS. Review of Tissue Simulating Phantoms for Optical Spectroscopy, Imaging and Dosimetry. *J Biomed Opt* 2006; **11**(4): 041102.

29. De Grand AM, Lomnes SJ, Lee DS, Pietrzykowski M, Ohnishi S, Morgan TG, Gogbashian A, Laurence RG, Frangioni JV. Tissue-Like Phantoms for Near-Infrared Fluorescence Imaging System Assessment and the Training of Surgeons. *J Biomed Opt* 2006; **11**(1): 014007.

30. Yuan B, Chen N, Zhu Q. Emission and Absorption Properties of Indocyanine Green in Intralipid Solution. *J Biomed Opt* 2004; **9**(3): 497-503.

31. Lizuka MN, Sherar MD, Vitkin IA. Optical Phantom Materials for Near Infrared Laser Photocoagulation Studies. *Lasers Surg Med* 1999; **25**(2): 159-69.

32. Durkin AJ, Jaikumar S, Richardskortum R. Optically Dilute, Absorbing, and Turbid Phantoms for Fluorescence Spectroscopy of Homogeneous and Inhomogeneous Samples. *Appl Spectrosc* 1993; **47**(12): 2114-21.

33. Wagnieres G, Cheng S, Zellweger M, Utke N, Braichotte D, Ballini JP, van den BH. An Optical Phantom With Tissue-Like Properties in the Visible for Use in PDT and Fluorescence Spectroscopy. *Phys Med Biol* 1997; **42**(7): 1415-26.

34. Intes X. Time-Domain Optical Mammography SoftScan: Initial Results. *Acad Radiol* 2005; **12**(8): 934-47.

35. Berridge DL, Mastey LA, Eckstrom PC, Czarnecki DJ. Indocyanine Green Dye As a Tissue Marker for Localization of Nonpalpable Breast Lesions. *AJR Am J Roentgenol* 1995; **164**(5): 1299.

36. Ke S, Wen X, Gurfinkel M, Charnsangavej C, Wallace S, Sevick-Muraca EM, Li C. Near-Infrared Optical Imaging of Epidermal Growth Factor Receptor in Breast Cancer Xenografts. *Cancer Res* 2003; **63**(22): 7870-5.

37. Mieog JS, Hutteman M, van dV, Jr., Kuppen PJ, Que I, Dijkstra J, Kaijzel EL, Prins F, Lowik CW, Smit VT, van d, V, Vahrmeijer AL. Image-Guided Tumor Resection Using Real-Time Near-Infrared Fluorescence in a Syngeneic Rat Model of Primary Breast Cancer. *Breast Cancer Res Treat* 2010.

BCS	Breast-conserving surgery
BCT	Breast-conserving therapy
FDA	Food & drug administration
FRI	Fluorescence reflectance imaging
FWHM	Full width at half maximum
HCl	Hydrochloric acid
ICG	Indocyanine green
NIR	Near-infrared
NIRF	Near-infrared fluorescence
SLN	Sentinel lymph node
SN	Signal-to-noise
TBS	Tris-buffered saline